Physics Letters A 375 (2011) 1023–1027

Contents lists available at ScienceDirect

Physics Letters A

www.elsevier.com/locate/pla

Anisotropic pairing symmetry effect on crossed Andreev reflection in a graphene-based transistor

Chunxu Bai [a,*], Juntao Wang [b], Yanling Yang [a]

[a] School of Physics, Anyang Normal University, Anyang 455000, China
[b] Department of Mathematics, Henan Institute of Science and Technology, Xinxiang 453000, China

ARTICLE INFO

Article history:
Received 21 December 2010
Accepted 30 December 2010
Available online 5 January 2011
Communicated by V.M. Agranovich

Keywords:
Graphene
Crossed Andreev reflection
Anisotropic pairing symmetry

ABSTRACT

Crossed Andreev reflection (CAR) under the influence of anisotropic pairing symmetry is considered. It is shown that CAR is sensitive to the Fermi energy and the orientation of the gap. In addition, the oscillatory period of CAR can be not only tunable by the potential energy in the superconductor region, it also can be modulated by the length of the superconductor region. The physical origination for those phenomena has also been analyzed.

1. Introduction

Almost fifty years ago, the low-energy spectrum in graphene, a monatomic layer of carbon atoms arranged on a honeycomb lattice, was formally described by Slonczewski and Weiss [1]. However, the real breakthrough on graphene research came with Novoselov et al.'s report of experimental acquisition of graphene flakes by a simple piece of adhesive tape [2]. It was this work which bridged the gap between experimental observation and the theoretical framework as the theoretical examples of two dimension materials. Since the pioneering work of Novoselov et al., the study of graphene flakes has progressed rapidly [3,4]. Because of unique linear dispersion relation in graphene, several novel phenomena were found in the materials, such as unconventional quantum Hall effect [5,6], strong electric-field effect [7], finite minimal conductivity [5,8], Klein paradox [9] and so on.

In particular, since the specular Andreev reflection (SAR) was found by Beenakker in 2006 [10], the physical properties of graphene-based superconductor junction have attracted great interest due to its novel features and potential applications in future electronic circuits [3,4]. Theoretically, novel propagating modes of Andreev electrons [11], oscillation of tunneling probability with barrier width [12], and a pure crossed Andreev reflection (CAR) [13] have been revealed in recent years. Furthermore, CAR effect on magnetoresistance, shot noise, and spin-valves effect has also been extensively investigated by many authors [14–16]. Experimentally, the observation of bi-polar supercurrent and multiple Andreev reflection in graphene Josephson junction has been reported by several groups [17–19].

Graphene is not a natural superconductor. Those graphene-based superconductor leads are fabricated by means of depositing superconducting leads on a graphene flake. Thus, except of the conventional s-wave superconducting pairing which is the primary focus above, the unconventional pairing in graphene-based superconductor leads could be achieved by proximity effect through an unconventional superconductor lead, such as high-Tc superconductor. Consequently, some attention has been paid to how unconventional pairing would affect coherent quantum transport in graphene-based superconductor junction [20,21]. It is found that the zero-bias conductance peak only forms at the orientation of the gap in k-space with regard to the interface which is very close to $\pi/4$ and the Josephson current exhibits a weakly-damped, oscillatory dependence on the length of the junction. Indeed, those results indicate that the effect of anisotropic pairing symmetry on the quantum transport properties in a graphene-based superconductor junction is of considerable importance.

However, all these investigations about the unconventional superconductors only focus on two-terminal device. It is interesting to ask what kinds of new features emerge when the CAR effect is regulated by the anisotropic pairing symmetry. Moreover, what's the relationship between the crossed specular Andreev reflection (CSAR) and the anisotropic pairing symmetry is more important, since the unusual effect-specular Andreev reflection is never observed in the conventional material. To the end, in this Letter, we investigate the CAR in a three-terminal graphene-based superconductor transistor based on the Dirac–Bogoliubov–de Gennes

* Corresponding author. Tel.: +86 372 2900041; fax: +86 372 2900041.
E-mail address: chunxu_bai@yahoo.cn (C. Bai).

0375-9601/$ – see front matter
doi:10.1016/j.physleta.2010.12.080

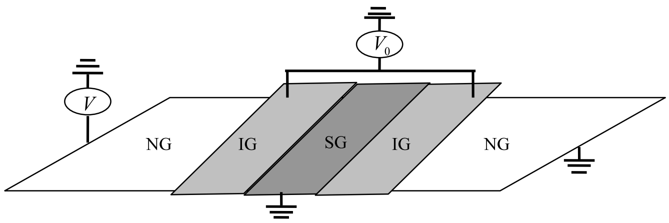

Fig. 1. Schematic diagram of the three-terminal *NG/IG/SG/IG/NG* transistor.

(DBdG) equation. The CAR and the non-local conductivity of this system will be calculated, and the relationship between the CSAR and the anisotropic pairing symmetry will be discussed. The rest of the Letter is organized as follows: we will describe the theory and method in Section 2, present the results and discussion in Section 3, and give a summary in Section 4.

2. Theory and model

We consider a three-terminal normal/insulator/superconductor/insulator/normal (*NG/IG/SG/IG/NG*) transistor in a monolayer graphene membrane occupying the xy plane, and the schematic setting is shown in Fig. 1. Here the left and right leads are made of the same *NG*, and they are separated from the central *SG* by two identical thin barriers, respectively. The leads *IG*, modeled by a gate voltage, extend from $x=-d$ to $x=0$ and $x=l$ to $x=l+d$ while the *SG* lead occupies $0<x<l$. Such a local barrier can be realized by either using the electric field effect or local chemical doping [2]. The superconductivity is induced in region $0<x<l$ via the proximity effect, where the graphene membrane is to be kept close to an unconventional superconductive lead (such as high-Tc superconductor) so that it can generate a d-wave pairing symmetry in this region [3,4,10–21]. In the following, we focus on the case where the width (along y direction) of the graphene strip, w, is much larger than d and l. Thus, the details of microscopic description of the strip edges become irrelevant, and can be realistically implemented in experiments [2]. The potential profile $V(x)$ in regions *NG*, *IG*, and *SG* may be adjusted independently by a gate voltage or doping, which is taken as

$$V(x)=\begin{cases}0, & x<-d,\ x>l+d,\\ -U_0, & 0<x<l,\\ V_0, & -d<x<0,\ l<x<l+d.\end{cases} \tag{1}$$

For the *SG* lead, neglecting the self-consistency of the superconducting pair potential, $\Delta(x)$ is taken in the form $\Delta(x)=\Delta_0\cos(2\theta_S-2\alpha)e^{i\varphi}\theta(x)$, where $\theta(x)$ is the Heaviside step function, Δ_0 and φ are the maximum amplitude and the phase of the induced superconductive order parameter, respectively, α models the orientation of the gap in k-space with regard to the interface, and θ_S is the transmission angle between the momentum of the quasiparticle and the x axis. Here we consider the case where the superconducting coherence length is larger than the wave length in the superconducting region, namely $0\ll V_0$. The low energy quasiparticles in the present system can be described by the following DBdG equation [10]

$$\begin{pmatrix} H_a-E_F & \Delta(r)\\ \Delta^*(r) & E_F-H_a\end{pmatrix}\Psi_a=E\Psi_a \tag{2}$$

where $\Psi_a=(\Psi_{Aa},\Psi_{Ba},\Psi^*_{A\bar{a}},-\Psi^*_{B\bar{a}})$ are the 4 component wave functions for the electron and hole spinors, the index a denotes K or K' for electrons or holes near K and K' points, $\bar{a}$ takes value $K'(K)$ for $a=K(K')$, E_F denotes the Fermi energy, A and B denote the two inequivalent sites in the hexagonal lattice of graphene, and the Hamiltonian H_0 is given by

$$H_0=-i\hbar v_F\left[\sigma_x\partial_x+\mathrm{sgn}(a)\sigma_y\partial_y\right]+V(x) \tag{3}$$

where v_F denotes the Fermi velocity of the quasiparticle in graphene, $V(x)$ represents the electrostatic potential in the five leads, and $\mathrm{sgn}(a)$ takes value $+(-)$ for $a=K(K')$.

In order to solve the transport problem in our *NG/IG/SG/IG/NG* transistor (sketched in Fig. 1), we assume that the electron or hole wave propagates at an angle ϕ or ϕ' along x axis. For an electron with an energy ε and transverse momentum q incident on the transistor from the left *NG* lead (as shown in Fig. 1), taking into account both Andreev and normal reflection processes in the left *NG* lead ($x<-d$) and both elastic co-tunneling and Andreev transmission processes in the right *NG* lead ($x>l+d$), the wave functions in the five regions can be written as [14,15]

$$\begin{aligned}
&\Psi_1=\Psi_N^{e+}+r\Psi_N^{e-}+r_A\Psi_N^{h-},\\
&\Psi_2=p_1\Psi_I^{e+}+q_1\Psi_I^{e-}+m_1\Psi_I^{h+}+n_1\Psi_I^{h-},\\
&\Psi_3=e\Psi_S^{e+}+f\Psi_S^{h+}+g\Psi_S^{e-}+h\Psi_S^{h-},\\
&\Psi_4=p_2\Psi_I^{e+}+q_2\Psi_I^{e-}+m_2\Psi_I^{h+}+n_2\Psi_I^{h-},\\
&\Psi_5=t\Psi_N^{e+}+t'\Psi_N^{h+},
\end{aligned} \tag{4}$$

where r and r_A are the amplitudes of normal and Andreev reflections in the left *NG* region, respectively, t and t' are the amplitudes of elastic co-tunneling and Andreev transmission processes in the right *NG* region, respectively, $p_{1,2}$, $q_{1,2}$, $m_{1,2}$, and $n_{1,2}$ are the amplitudes of electron and hole in the *IG* region, and e, f, g, and h are the amplitudes of electron-like and hole-like quasiparticles in the *SG* region.

The wave function in Eq. (4) can be expressed clearly by the solution of Eq. (2). In the *NG* region, the wave functions are given by

$$\begin{aligned}
&\Psi_N^{e\pm}=\left(1,\pm e^{\pm i\phi},0,0\right)e^{i(\pm k_N x+qy)},\\
&\Psi_N^{h\pm}=\left(0,0,1,\mp e^{i(\pm i\phi')}\right)e^{i(\pm k'_N x+qy)},\\
&\sin(\phi)=\hbar v_F q/(\varepsilon+E_F),\\
&\sin\left(\phi'\right)=\hbar v_F q/(\varepsilon-E_F),
\end{aligned} \tag{5}$$

where $\Psi_N^{e\pm}$ and $\Psi_N^{h\pm}$ are the wave functions traveling along the $\pm x$ direction with a transverse momentum $k_y=q$ and an energy ε for electron and hole, respectively, and $k_N=(\varepsilon+E_F)\times\cos(\phi)/\hbar v_F$, $k'_N=(\varepsilon-E_F)\times\cos(\phi')/\hbar v_F$ are the momentum along the x axis. Note that the critical incident angle should be considered in the scattering process, and it is given by $\phi_C=\arcsin[|k'_N|/k_N]$. When the incident angle of the quasiparticle is larger than the critical angle ($|\phi|>\phi_C$), one should take $\phi'=\mathrm{sgn}(\phi)(\frac{\pi}{2}\,\mathrm{sgn}(k'_N)-iar\cosh|\frac{\sin\phi}{\sin\phi_C}|)$. However, the evanescent solutions in the calculations for such a case have to be included to ensure the current conservation.

In the *IG* region, one can also obtain $\Psi_I^{e\pm}=(1,\pm e^{\pm i\beta},0,0)\times e^{i(\pm k_I x+qy)}$ and $\Psi_I^{h\pm}=(0,0,1,\mp e^{\pm i\beta'})e^{i(\pm k'_I x+qy)}$ for electron and hole moving along $\pm x$. Here the angle of incidence of the electron (hole) $\beta(\beta')$ is defined as $\sin[\beta(\beta')]=\hbar v_F q/[\varepsilon+(-)(E_F-V_0)]$ and $k_I(k'_I)=[\varepsilon-(+)(E_F-V_0)]\cos[\beta(\beta')]/\hbar v_F$. Note that in the limit of a thin barrier (where $V_0\to\infty$ and $d\to 0$, but $\chi=V_0 d/\hbar v_F$ remains finite), β, $\beta'\approx 0$ and $-k_I d$, $k'_I d\approx\chi$.

In the *SG* region, the wave functions of the DBdG quasiparticles can be shown in the same way as

$$\begin{aligned}
\Psi_S^{e\pm}=&\left(u\left(\theta^+\right),\pm u\left(\theta^+\right)e^{\pm i\theta^+},v\left(\theta^+\right)e^{-i\varphi^+},\right.\\
&\left.\pm v\left(\theta^+\right)e^{i\left(\pm\theta^+-\varphi^+\right)}\right)e^{i(\pm k_S^e x+qy)},\\
\Psi_S^{h\pm}=&\left(v\left(\theta^-\right),\pm v\left(\theta^-\right)e^{\pm i\theta^-},u\left(\theta^-\right)e^{-i\varphi^-},\right.\\
&\left.\pm u\left(\theta^-\right)e^{i\left(\pm\theta^--\varphi^-\right)}\right)e^{i(\pm k_S^h x+qy)},
\end{aligned} \tag{6}$$

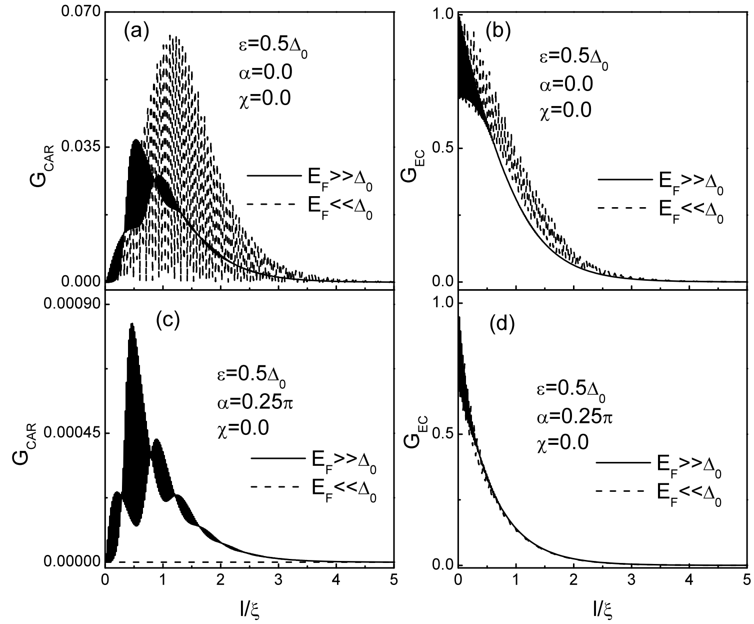

Fig. 2. (a) and (c) represent G_{CAR} for the three-terminal *NG*/*IG*/*SG*/*IG*/*NG* transistor; (b) and (d) correspond to G_{EC} for the three-terminal *NG*/*IG*/*SG*/*IG*/*NG* transistor. Solid line and dashed line correspond to $E_F \gg \Delta_0$ and $E_F \ll \Delta_0$, respectively. The other parameters are shown in the figure.

where $k_S^{e(h)} = (U_0 + E_F + (-)\sqrt{\varepsilon^2 - |\Delta(\theta^{+(-)})|^2}) \cos\theta^{+(-)}/(\hbar v_F)$, the coherence factors are given by

$$u(\theta) = \sqrt{\left(1 + \sqrt{\varepsilon^2 - \left|\Delta(\theta)\right|^2/\varepsilon}\right)/2},$$

$$v(\theta) = \sqrt{\left(1 - \sqrt{\varepsilon^2 - \left|\Delta(\theta)\right|^2/\varepsilon}\right)/2},$$

$$\theta^{+(-)} = \theta_S^e\left(\pi - \theta_S^h\right),$$

and $e^{i\varphi^{\pm}} = \Delta(\theta^{\pm})/|\Delta(\theta^{\pm})|$. The transmission angle $\theta_S^{e(h)}$ for the electron-like (hole-like) quasiparticle is defined as $\frac{\sin\theta^{e(h)}}{\sin\phi} = \frac{(\varepsilon+E_F)}{(U_0+E_F+(-)\sqrt{\varepsilon^2-|\Delta(\theta^{e(h)})|^2})}$.

All the amplitudes in Eq. (4) can be determined by demanding wave function continuity at the interfaces:

$$\psi_1(-d) = \psi_2(-d), \qquad \psi_2(0) = \psi_3(0),$$
$$\psi_3(l) = \psi_4(l), \qquad \psi_4(l+d) = \psi_5(l+d). \tag{7}$$

After the transmission coefficients are obtained, we can discuss the non-local conductivity. Concerning the non-local conductance calculation in graphene-based *s*-wave superconductor junction, the situation is exploited rapidly [13–16]. It is shown that they have already hold some advantage towards the implementation of spin-entangled states of the electron in comparison with the conventional one. Now, we extend these discussions to the *NG*/*IG*/*SG*/*IG*/*NG* system with an anisotropic pairing symmetry (*d*-wave pairing symmetry). The non-local conductivity (G_C) is defined by the difference between the crossed Andreev conductivity (G_{CAR}) and electronic co-tunneling conductivity (G_{EC}),

$$G_C = G_{CAR} - G_{EC}. \tag{8}$$

Here, G_{CAR} and G_{EC} are expressed as [15]

$$G_{CAR} = G_0 \int_{-\pi/2}^{\pi/2} \left|t'\right|^2 \cos(\phi')\, d\phi \quad \text{and}$$

$$G_{EC} = G_0 \int_{-\pi/2}^{\pi/2} |t|^2 \cos(\phi)\, d\phi, \tag{9}$$

where $G_0 = 4e^2 N(eV)/h$ is the ballistic conductivity of the graphene, eV is the bias voltage, and $N(eV) = (\varepsilon + E_F)w/(\pi\hbar v_F)$ denotes the numbers of available channels for the graphene sample with width w. Based on Eqs. (8) and (9) three kinds of conductivity (G_C, G_{CAR}, and G_{EC}) for our three-terminal transistor can be obtained easily by the numerical calculations.

3. Numerical results and discussion

We first calculate G_{CAR} and G_{EC} (without the insulating region) as a function of l in the two cases of $\alpha = 0$ (Fig. 2(a) and (b)) and $\alpha = \pi/4$ (Fig. 2(c) and (d)), and the results are plotted in Fig. 2. The solid lines and dashed lines represent the regime $E_F \gg \Delta$ and $E_F \ll \Delta$, respectively. Here we set the superconducting gap $\Delta_0 = 1$ and the other energy parameters are scaled in terms of Δ_0. The other parameters are denoted in the figures. In the case of $\alpha = 0$, the superconducting pair potential is taken as $\Delta(x) = \Delta_0 \cos(2\theta_S) e^{i\varphi}\theta(x)$, and the *d*-wave pair potential is essentially identical to the *s*-wave case, since $\Delta(\theta^+)$ and $\Delta(\theta^-)$ have the same sign independent of θ. Thus the previous results of the three-terminal graphene-based normal/insulator/*s*-wave superconductor/insulator/normal transistor are reproduced [15], as shown in Fig. 2(a) and (b). However, in the case of $\alpha = \pi/4$, there are some intriguing features summarized here. First, for G_{EC} (Fig. 2(d)), one might find that little divergence between $E_F \ll \Delta$ and $E_F \gg \Delta$, which is different from the case of $\alpha = 0$. On the other hand, although G_{EC} decreases almost monotonically from a peak at $l = 0$ which is similar to the case of $\alpha = 0$, but the magnitude of G_{EC} decays rapidly as an exponential form with the distance l between the leads on a scale fixed by the superconducting coherence length ξ. Second, as seen from Fig. 2(c), unlike G_{EC}, G_{CAR} is sensitive to the change of E_F. That is to say, for $E_F \gg \Delta_0$ where only the CAR takes place, G_{CAR} reaches its maximum around $l \sim \xi$, and vanishes for $l = 0$ and $l \gg \xi$. While, for $E_F \ll \Delta_0$ where only the CSAR takes place, the value of G_{CAR} always equates to a negligible value although it has a similar structure as the case of

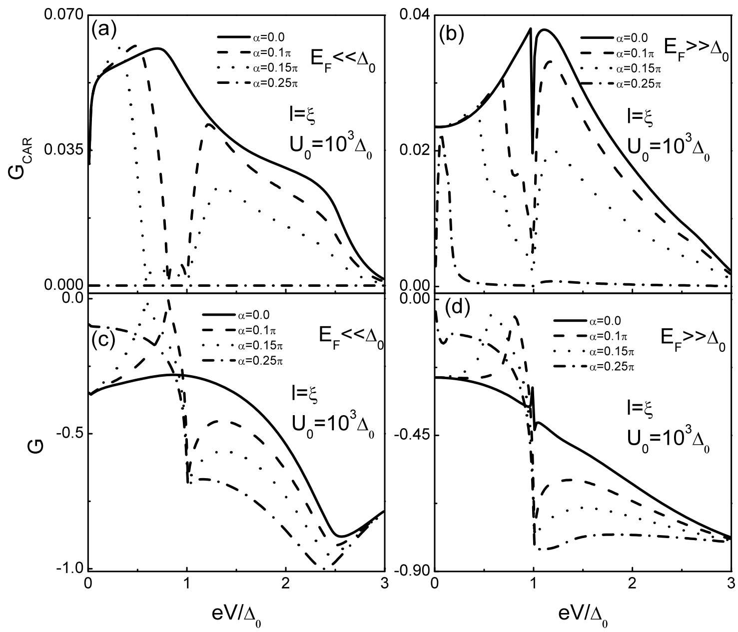

Fig. 3. (a) and (b) represent G_{CAR} for the *NG*/*IG*/*SG*/*IG*/*NG* transistor; (c) and (d) correspond to G for the *NG*/*IG*/*SG*/*IG*/*NG* transistor. The parameters are shown in the figure.

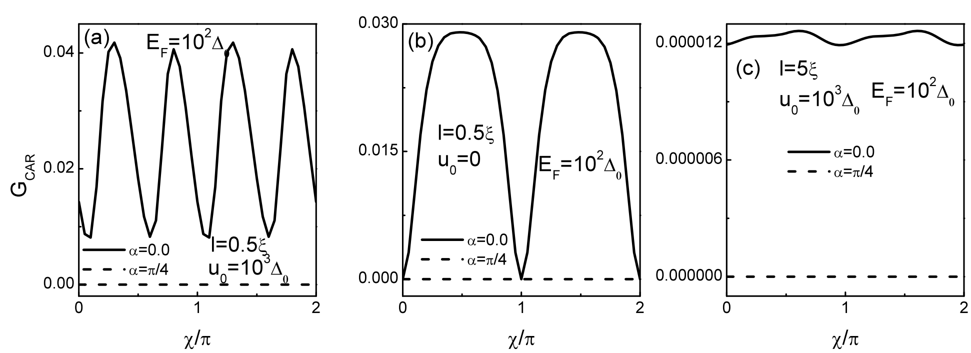

Fig. 4. Zero-bias G_{CAR} for the *NG*/*IG*/*SG*/*IG*/*NG* transistor as a function of χ. The solid lines and dashed lines represent $\alpha = 0$ and $\alpha = \pi/4$, respectively. We set $l = 0.5\xi$ and $U_0 = 10^3\Delta_0$ in (a), $l = 0.5\xi$ and $U_0 = 0$ in (b), and $l = 5\xi$ and $U_0 = 10^3\Delta_0$ in (c).

$E_F \gg \Delta_0$. Meanwhile, by comparing the values of G_{CAR} of $\alpha = 0$ and of $\alpha = \pi/4$, we can conclude that the angle α has a suppressed effect on G_{CAR} for $0 \leqslant \alpha \leqslant \pi/4$. Physically, the maximum contribution of G_{CAR} occurs when the modulus of the pair potential is maximum. Since G_{CAR} is an integral quantity, the key contribution of G_{CAR} is obtained when the electron is incident on the interface normally. Thus, G_{CAR} reaches its maximum when $\alpha = 0$ but is suppressed to a negligible value when $\alpha = \pi/4$.

For the next step, we will investigate how G_{CAR} and G (without the insulating region) will change when the orientation of superconductor gap varies from $\alpha = 0$ to $\alpha = \pi/4$, and the results are plotted in Fig. 3. The solid lines, dashed lines, dotted lines, and dashed–dotted lines represent $\alpha = 0$, $\alpha = 0.1\pi$, $\alpha = 0.15\pi$, and $\alpha = \pi/4$, respectively. The parameters used in the calculation are shown in the figure. Intuitively, for $\alpha = 0$, one might find that a minimal divergence of G_{CAR} occurs when eV is comparable in magnitude to Δ_0 [15]. In particular, for the case of CSAR ($E_F \ll \Delta_0$), this seems to be more justifiable since just like the case of a two-terminal junction where the local Andreev reflection reaches a certain value (a value smaller than 1), G_{CAR} can also reach an appropriate value but not equate to zero. We have verified that the result of $\alpha = 0$ would coincide with the result obtained by using the s-wave superconducting pairing when the wave vector $k_S^{e(h)} = (U_0 + E_F + (-)\sqrt{\varepsilon^2 - |\Delta(\theta^{+(-)})|^2}\,) \cos\theta^{+(-)}/(\hbar v_F)$ is substituted by $k_S^{e(h)} = (U_0 + E_F + (-)i\Delta_0) \cos\theta^{+(-)}/(\hbar v_F)$. We believe that this displacement may be acceptable for $eV \ll \Delta_0$, but unfit for the case of $eV \approx \Delta_0$. Furthermore, it is also important to note in Fig. 3(a) and (b) that the orientation of superconductor gap α plays an important role in G_{CAR}. As α changes from 0 to $\pi/4$, a dip of G_{CAR} is shown which centres at $eV = \Delta_0$. The amplitude of G_{CAR} is sharply reduced for $\alpha = \pi/4$ and $E_F \ll \Delta_0$ in the whole energy region. While for $\alpha = \pi/4$ and $E_F \gg \Delta_0$, a sharp peak is observed at $eV \sim 0$. One distinct feature is that, at $eV = 0$, G_{CAR} reaches a constant value as α increases from 0 to $\pi/4$, but only drops to zero for $\alpha = \pi/4$. Physically, this phenomenon is consistent with the conductivity in two-terminal devices calculated in Ref. [20]. At zero bias, for $\alpha = \pi/4$, a perfect zero-energy state forms at the interface of transistor which gives rise to a zero-bias conductance peak. Thus, for the three-terminal devices, G_{CAR} equates to zero when $eV = 0$ and $\alpha = \pi/4$. Fig. 3(c) and (d) show the calculated results of G. It means that G is dominated by electronic co-tunneling.

Finally, to investigate the effect of the barrier potential, zero-bias ($eV = 0$) G_{CAR} of the present transistor as a function of the barrier strength χ is calculated in Fig. 4. The parameters are denoted in the figure. It is clearly shown that the G_{CAR} for $\alpha = 0$ exhibits novel periodic oscillatory behavior as a function of χ. Basically, G_{CAR} for $\alpha = \pi/4$ always shows the same features as the case of $\alpha = 0$. However, due to its negligible value, it seems to be almost independent on χ which is shown in the figure. In particular, the oscillatory period can be tunable by the potential strengths U_0 in *SG*. That is to say, as shown in Fig. 4(b), G_{CAR} exhibits a π periodic oscillatory behavior as a function of χ for $U_0 = 0$ which recovers the results in Ref. [12]. However, the striking feature is that G_{CAR} exhibits a new $\pi/2$ periodic oscillatory behavior for $U_0/E_F = 10^3$ (in Fig. 4(a)), which is consistent with the study in Ref. [22]. This phenomenon can be intuitively understood from the fact that a large potential strength U_0 in *SG* acts as an additional effective barrier for the electron transport through the transistor. As a consequence, it leads to a new $\pi/2$ periodic oscillatory character for $U_0/E_F = 10^3$. Furthermore, the oscillatory period can be not only tunable by U_0, but also sensitive to the length of *SG*. Fig. 4(c) describes G_{CAR} as a function of χ at a large l ($l/\xi = 5$). The π periodic oscillatory behavior is observed again. Physically, the oscillation originates from the fact that the relativistic massless fermions with the purely real momenta may interfere in the barrier regions. For a large U_0 and a certain l, an coherent interference effect would be induced in *SG*. Therefore, it results in the change of the oscillatory period of G_{CAR} for this transistor. Whereas, for a large l, as the interference effect decay in *SG*, the present structures degenerate into the single junction case and then the results (in Fig. 4(c)) are identical with that in Ref. [12]. For G, it is also a periodic function of χ and behave like G_{CAR} (not plotted here).

4. Summary

Here we undertake a study for CAR through the three-terminal graphene-based superconductor transistor with the anisotropic pairing symmetry by using the DBdG equation. We have found that G_{CAR} is sensitive to the change of E_F due to the dominant of CAR or CSAR. Meanwhile, it is also sensitive to the orientation of the gap α. Furthermore, we have found that G_{CAR} exhibits a periodic oscillatory behavior as a function of χ. Especially, the oscillatory period can be not only tunable by U_0, but also can be modulated by the length of *SG*. The physical reason for those features has also been discussed.

References

[1] J.C. Slonczewski, P.R. Weiss, Phys. Rev. 109 (1958) 272.
[2] K.S. Novoselov, A.K. Geim, S.V. Morozov, D. Jiang, Y. Zhang, S.V. Dubonos, I.V. Grigorieva, A.A. Firsov, Science 306 (2004) 666.
[3] C.W.J. Beenakker, Rev. Mod. Phys. 80 (2008) 1337.
[4] A.H. Castro Neto, F. Guinea, N.M.R. Peres, K.S. Novoselov, A.K. Geim, Rev. Mod. Phys. 81 (2009) 109.
[5] K.S. Novoselov, A.K. Geim, S.V. Morozov, D. Jiang, M.I. Katsnelson, I.V. Grigorieva, S.V. Dubonos, A.A. Firsov, Nature 438 (2005) 197.
[6] Y. Zhang, Y.W. Tan, H.L. Stormer, P. Kim, Nature 438 (2005) 201.
[7] Y. Zhang, J.P. Small, M.E.S. Amori, P. Kim, Phys. Rev. Lett. 94 (2005) 176803.
[8] K.S. Novoselov, E. McCann, S.V. Morozov, V.I. Falko, M.I. Katsnelson, U. Zeitler, D. Jiang, F. Schedin, A.K. Geim, Nature Phys. 2 (2006) 177.
[9] M.I. Katsnelson, K.S. Novoselov, A.K. Geim, Nature Phys. 2 (2006) 620;
C. Bai, X. Zhang, Phys. Rev. B 76 (2007) 075430;
C. Bai, Y. Yang, X. Zhang, Phys. Rev. B 80 (2009) 235423.
[10] C.W.J. Beenakker, Phys. Rev. Lett. 97 (2006) 067007.
[11] M. Titov, A. Ossipov, C.W.J. Beenakker, Phys. Rev. B 75 (2007) 045417.
[12] S. Bhattacharjee, K. Sengupta, Phys. Rev. Lett. 97 (2006) 217001.
[13] J. Cayssol, Phys. Rev. Lett. 100 (2008) 147001.
[14] Y. Yang, C. Bai, D. Zhang, Eur. Phys. J. B 72 (2009) 217.
[15] C. Benjamin, J.K. Pachos, Phys. Rev. B 78 (2008) 235403.
[16] J. Linder, M. Zareyan, A. Sudbø, Phys. Rev. B 80 (2009) 014513.
[17] H.B. Heersche, P. Jarillo-Herrero, J.B. Oostinga, L.M.K. Vandersypen, A.F. Morpurgo, Nature 446 (2007) 56.
[18] X. Du, I. Skachko, E.Y. Andrei, Phys. Rev. B 77 (2008) 184507.
[19] F. Miao, S. Wijeratne, Y. Zhang, U.C. Coskun, W. Bao, C.N. Lau, Science 317 (2007) 1530.
[20] J. Linder, A. Sudbø, Phys. Rev. Lett. 99 (2007) 147001.
[21] J. Linder, A.M. Black-Schaffer, T. Yokoyama, S. Doniach, A. Sudbø, Phys. Rev. B 80 (2009) 094522.
[22] C. Bai, J. Wang, Y. Yang, Physica E 42 (2010) 1923.